

# Contribution of soil algae to the global carbon cycle

Vincent E. J. Jassey<sup>1</sup> , Romain Walcker<sup>1</sup> , Paul Kardol<sup>2</sup> , Stefan Geisen<sup>3,4</sup> , Thierry Heger<sup>5</sup> ,  
Mariusz Lamentowicz<sup>6</sup> , Samuel Hamard<sup>1</sup>  and Enrique Lara<sup>7</sup> 

<sup>1</sup>Laboratoire Écologie Fonctionnelle et Environnement, Université de Toulouse, CNRS, 31062 Toulouse, France; <sup>2</sup>Department of Forest Ecology and Management, Swedish University of Agricultural Sciences, 90183 Umeå, Sweden; <sup>3</sup>Laboratory of Nematology, Wageningen University, 6708 PB Wageningen, the Netherlands; <sup>4</sup>Department of Terrestrial Ecology, Netherlands Institute of Ecology NIOO-KNAW, 6708 PB Wageningen, the Netherlands; <sup>5</sup>Soil Science and Environment Group, Changins, HES-SO University of Applied Sciences and Arts Western, 1260 Nyon, Switzerland; <sup>6</sup>Climate Change Ecology Research Unit, Adam Mickiewicz University, 60-001 Poznań, Poland; <sup>7</sup>Real Jardín Botánico, CSIC, Plaza de Murillo 2, 28014 Madrid, Spain

## Summary

Author for correspondence:

Vincent E. J. Jassey

Email: [vincent.jassey@univ-tlse3.fr](mailto:vincent.jassey@univ-tlse3.fr)

Received: 4 November 2021

Accepted: 21 December 2021

*New Phytologist* (2022) **234**: 64–76

doi: 10.1111/nph.17950

**Key words:** biogeography, microbial photosynthesis, net primary productivity (NPP), photoautotrophs, soil carbon (C) cycle, soil microbiome.

• Soil photoautotrophic prokaryotes and micro-eukaryotes – known as soil algae – are, together with heterotrophic microorganisms, a constitutive part of the microbiome in surface soils. Similar to plants, they fix atmospheric carbon (C) through photosynthesis for their own growth, yet their contribution to global and regional biogeochemical C cycling still remains quantitatively elusive.

• Here, we compiled an extensive dataset on soil algae to generate a better understanding of their distribution across biomes and predict their productivity at a global scale by means of machine learning modelling.

• We found that, on average,  $(5.5 \pm 3.4) \times 10^6$  algae inhabit each gram of surface soil. Soil algal abundance especially peaked in acidic, moist and vegetated soils. We estimate that, globally, soil algae take up around 3.6 Pg C per year, which corresponds to *c.* 6% of the net primary production of terrestrial vegetation.

• We demonstrate that the C fixed by soil algae is crucial to the global C cycle and should be integrated into land-based efforts to mitigate C emissions.

## Introduction

Soils are a critical component of the global carbon (C) cycle and are paramount in mitigating climate change (Amelung *et al.*, 2020). They are the largest repository of organic matter on land, storing *c.* 1500 Gt C, which largely exceeds the amount of C stored in the aboveground vegetation (i.e. *c.* 560 Gt; Crowther *et al.*, 2019). The magnitude of the soil organic C pool depends strongly upon microorganisms, as microbial growth and activity balance the accumulation and release of organic C through the decomposition of plant litter (C. Liang *et al.*, 2017). To date, research on soil microorganisms has focused mostly on heterotrophic microbes and their role in C release, with less attention paid to the role of microbial photosynthesis in soil C inputs. Yet, many soil microorganisms are capable of CO<sub>2</sub> fixation (Šantrůčková *et al.*, 2018; Crowther *et al.*, 2019; Akinyede *et al.*, 2020; Oliverio *et al.*, 2020; Bay *et al.*, 2021) and might, therefore, contribute to soil C fluxes. In particular, whereas microbial photosynthesis in aquatic systems can quantitatively rival that of terrestrial plants (Field *et al.*, 1998), microbial C fixation in soils has so far never been evaluated at a global scale – but see Elbert *et al.* (2012) for partial estimations based on cryptogam ground cover.

Recent global studies characterizing soil biodiversity have shown that microorganisms capable of CO<sub>2</sub> fixation are

omnipresent in soil (Cano-Díaz *et al.*, 2020; Oliverio *et al.*, 2020; Bay *et al.*, 2021). Soil photoautotrophic microbes that fix atmospheric CO<sub>2</sub> through photosynthesis are often referred to as soil algae, whereas others perform CO<sub>2</sub> fixation using chemoautotrophy or heterotrophy via several metabolic pathways and reactions (Miltner *et al.*, 2004). The role of nonphototrophic CO<sub>2</sub> fixation in soil C balance has been increasingly studied in the past few years (Miltner *et al.*, 2004, 2005; Šantrůčková *et al.*, 2018; Spohn *et al.*, 2019; Akinyede *et al.*, 2020). However, soil algae often constitute a small proportion of the soil microbiome biomass (Mitchell *et al.*, 2003; Jassey *et al.*, 2013); for this reason, they are often seen as insignificant for soil C uptake – but see Yuan *et al.* (2012), Wu *et al.* (2015), and Ge *et al.* (2016). Yet, soil algae occur in a range of surface soils, such as forest, grassland, and desert soils (Cano-Díaz *et al.*, 2020; Oliverio *et al.*, 2020), and encompass myriads of prokaryotes and micro-eukaryotes, with Cyanobacteria and Chlorophyta being the most commonly reported phyla in soil diversity surveys (Cano-Díaz *et al.*, 2020; Oliverio *et al.*, 2020).

Soil algae have been extensively studied in drylands, where photoautotrophic biocrusts often constitute the main source of C for the soil system (Maier *et al.*, 2018). However, very few studies have considered the importance of soil C inputs by microscopic algae in other ecosystems (Wyatt *et al.*, 2011; Yuan *et al.*, 2012;

Schmidt *et al.*, 2016; Halvorson *et al.*, 2019; Hamard *et al.*, 2021a). Despite their apparent global distribution, our understanding of the ecological preferences of soil algae across broad spatial scales remains limited. Though some previous work has suggested that soil moisture availability is a key driver of soil algal net primary productivity (NPP) (Brostoff *et al.*, 2005; Yoshitake *et al.*, 2010; Hamard *et al.*, 2021a,b), other studies have highlighted the importance of temperature (Shimmel & Darley, 1985; Dettweiler-Robinson *et al.*, 2018) or plant community composition (Hamard *et al.*, 2021a), and it remains unclear how predictable soil algal NPP is at larger spatial scales. As a result, quantitative information on soil algal C fixation remains mostly restricted to drylands (Rodríguez-Caballero *et al.*, 2018) and is not readily available at the global scale. Generating quantitative, spatially explicit information about the distribution and productivity of soil algae at a global scale is thus critical for understanding microbial control over soil C dynamics, from contributions to soil C uptake to soil C stabilization and sequestration (C. Liang *et al.*, 2017).

In this study, we address a set of fundamental questions to advance our understanding of the importance of soil algae in the soil C cycle: What are the habitat preferences of soil algae? How predictable is the CO<sub>2</sub> fixation rate of soil algae across large spatial scales and environmental gradients? What is the contribution of soil algae to ecosystem C uptake? To address these questions, we collated data on soil algal abundance and NPP from 203 georeferenced locations in all major terrestrial biomes (Fig. 1a; Supporting Information Tables S1, S2). We first conducted a biome-level analysis to reveal the main patterns of soil algal abundance and NPP. Second, we identified the main drivers of the abundance and NPP of soil algae across biomes by using a stack of 55 global layers of climate, soil, and vegetation characteristics (Table S3). Finally, we used geospatial machine learning (ML) to generate a global, 1 km resolution map of soil algal net C fixation across the globe and estimated their global contribution to terrestrial NPP.

## Materials and Methods

### Literature survey

We collected data on soil algae from previously published studies and unpublished data collections using a systematic review approach. We searched for studies that quantified the density and/or Chl biomass and/or primary productivity of soil algae in surface soils. Peer-reviewed publications were collected by searching Web of Science (1 January 1970 to 10 November 2019), Google Scholar (1 January 1970 to 10 November 2019), and ResearchGate to construct our datasets for a period of 7 months (January–June 2019, with updates in November 2019). We used the keywords ‘soil algae’ OR ‘photoautotroph’ AND ‘biomass’ OR ‘abundance’ AND ‘photosynthesis’ OR ‘primary productivity’ to build our database on soil algal abundance, Chl biomass, and primary productivity in different types of ecosystems. We standardized our efforts by focusing on studies in which samples were taken from uppermost centimeters soil, including litter, as soil algae further down in the soil column are expected to have

only very small photosynthetic rates. For experimental studies, only the controls were considered.

### Data collection

After initial screening, PDFs of all papers were manually screened to collect data. In order to be suitable for our analyses, the chosen papers had to present (or make reference to) the following information and data:

- (1) Sampled soil algal communities using standard methodologies, which would adequately capture quantitative information of the abundance per g of dry soil, such as cytometry information, or the C-analyzer used to quantify primary productivity. At a minimum, total abundance or Chl biomass or primary productivity of algae at each site had to be measured. Ideally, there was information on the microbial domain (prokaryotes and/or eukaryotes), with the abundance data (cell counts) of each domain.
- (2) Information on the habitat cover and/or type of ecosystem.
- (3) Available geographic coordinates for all sampled sites, or maps that could be georeferenced. When spatial coordinates were absent, but the type of ecosystem present, we included these data in Fig. 1 but not in further calculations from Figs 2–4.

Data were extracted from tables, figures, the main text, and/or supplementary materials; data extraction from figures was performed using Web Plot Digitizer software (<https://automeris.io/WebPlotDigitizer/>). When multiple values were available in each study, we used the mean in our data analyses. Similarly, when only minimum and maximum values were reported, we used the mean between these two values. Information (including publication year, site location, number of plots, and ecosystem types) was extracted from a total of 166 publications. This resulted in a final subset of 203 georeferenced sites and 19 nongeoreferenced sites that were used for further analyses. These sites include a wide range of ecosystem types (forests, grasslands, croplands, and wetlands) and climatic regions (arid, temperate, tropical, continental, and polar ecosystems), which we classified into seven biomes: grasslands (6.4% of the data), drylands (19.7%), broadleaf and mixed forests (14.3%), alpine and polar lands (20.7%), wetlands (15.3%), croplands (11.8%), and broadleaf evergreen forests (11.8%; see Tables S1, S2 for details).

### Data collation

The data taken from one publication, including supplementary material, or from our own unpublished measurements were considered as a ‘dataset’. For each dataset, we calculated the following site-level community metrics where possible: total (prokaryotes + micro-eukaryotes) abundance of soil algae per g of dry soil at the site, and soil algal net C uptake ( $\text{g C m}^{-2} \text{yr}^{-1}$ ) at the site level. Issues often arose when compiling data from different studies as the estimate may depend on the methods used. Therefore, we referenced the methodologies used for quantifying soil algal abundance and/or NPP for each dataset.

Three methods for quantifying the abundance of soil algae in surface soils were reported in our database: culture dependent through counting colony-forming units (CFUs; 34% of the data;

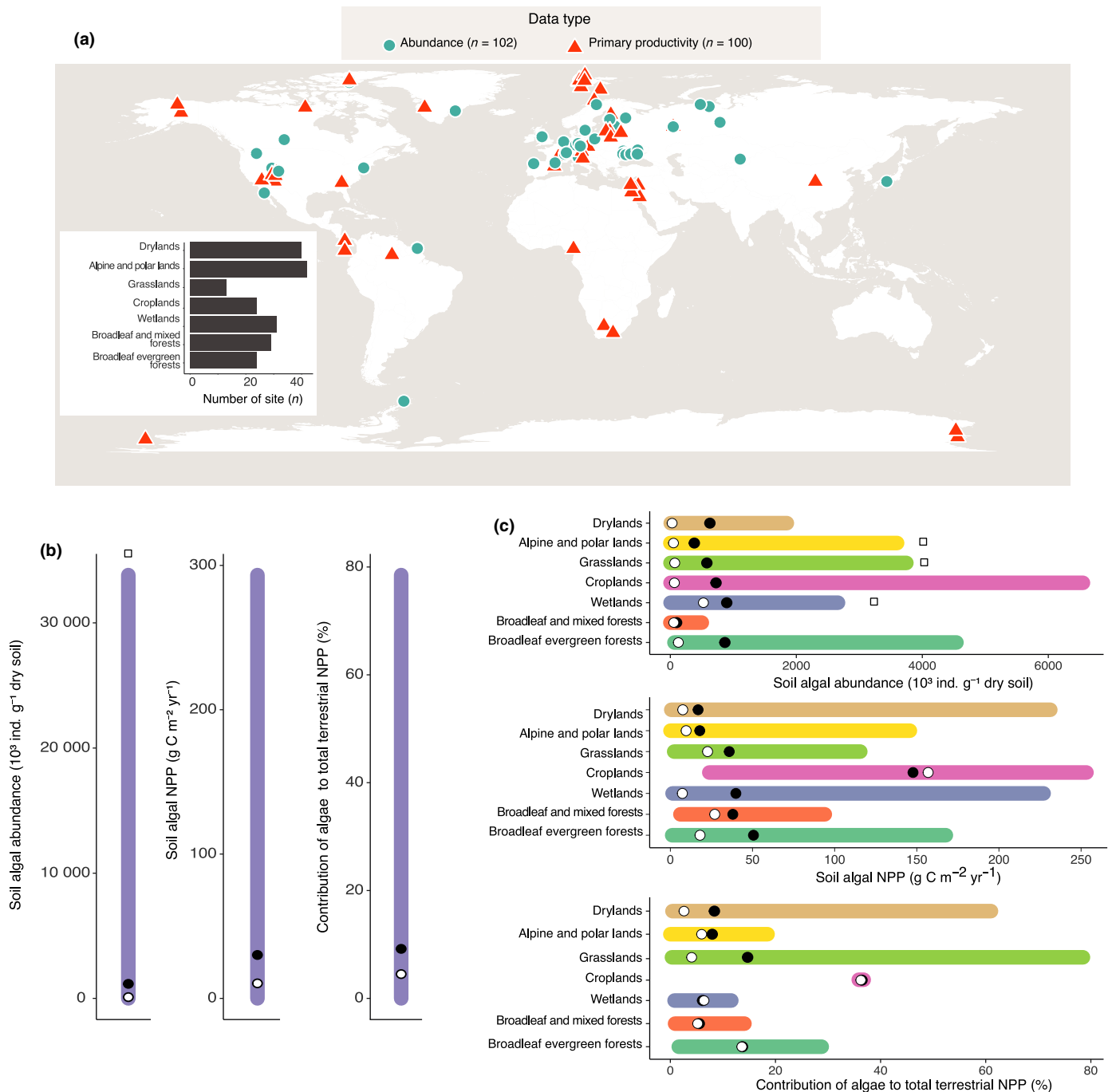


**Fig. 1** Sample locations and abundance, annual net primary productivity (NPP) and contribution of soil algae to total NPP. (a) A total of 203 georeferenced data points were collected from the literature and unpublished data and grouped into biome categories. (b, c) Averaged soil algal abundance ( $n = 101$ ), NPP ( $n = 102$ ), and contribution to total NPP ( $n = 100$ ): (b) overall; (c) per biome category. Open circles represent the mean and filled circles the median. Colored bars indicate the range between the minimum and maximum values. Little squares indicate clipped extreme values; one clipped value in (b) and three clipped values in (c). These extremely high values have been removed to increase the readability of means and medians.

only prokaryotes), flow cytometry (12%), and direct microscopy (54%). These three techniques measure living and active cells only, but their respective limitations – see details in Maron *et al.* (2006), Kallmeyer *et al.* (2008), and Beal *et al.* (2020) – may have influenced the final estimate of soil algal abundance. Although these techniques give similar trends (Beal *et al.*, 2020), CFUs may overestimate cyanobacterial counts as this method selects for

rapid-growing specimens, whereas flow cytometric and microscopic cell counting may underestimate densities as they require detachment and mechanical or optical separation of cells from interfering soil inorganic particles (Maron *et al.*, 2006). To test the potential bias in our data, we performed a linear mixed effects model with the method used as a fixed effect and microbial domain nested into ecosystem type and latitude as random effect

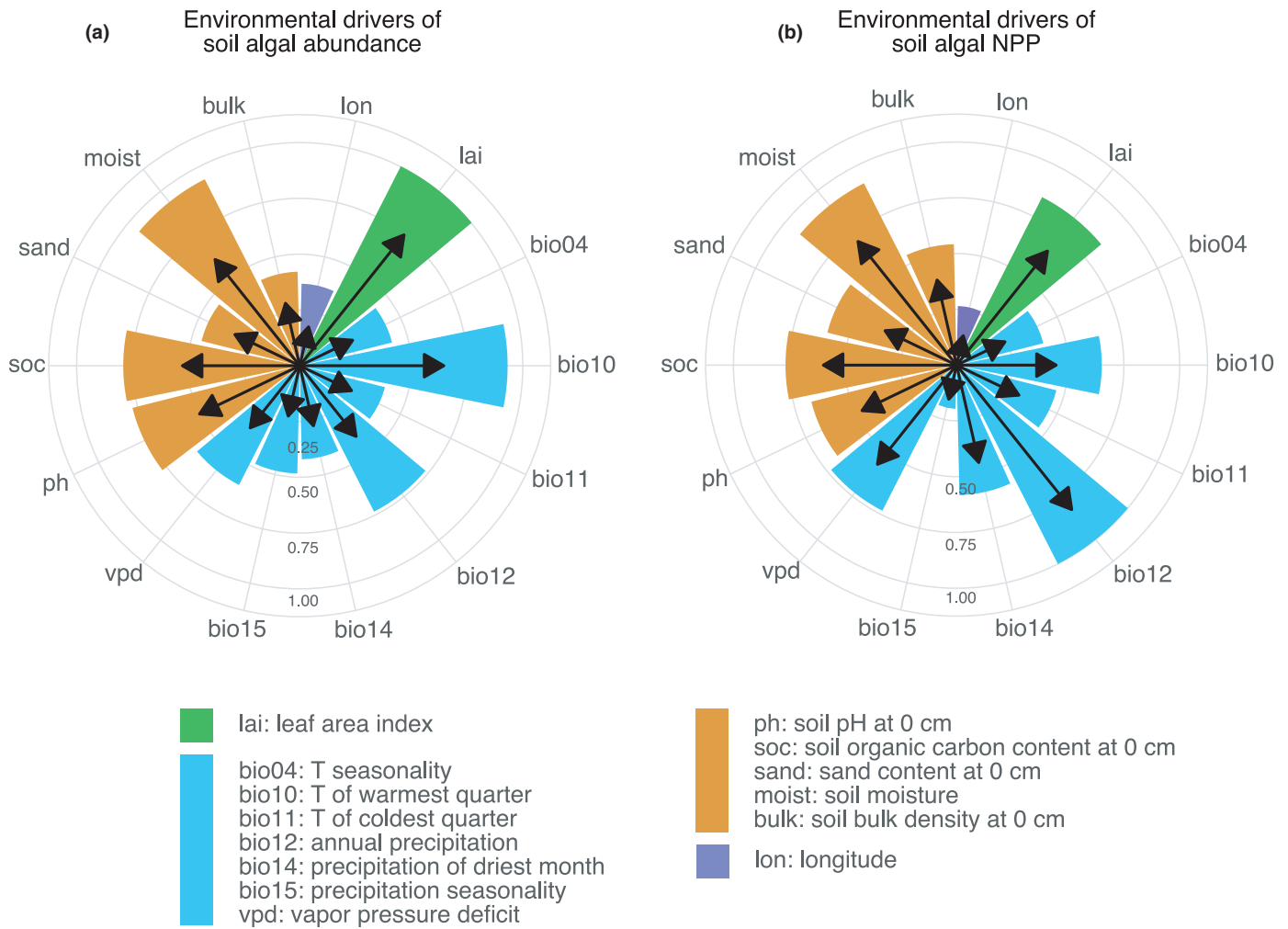


**Fig. 2** Environmental factors controlling the abundance and net primary productivity (NPP) of soil algae. Results from Boruta algorithm evaluating the relevance of different environmental predictors for (a) the abundance and (b) the NPP of soil algae. Arrow length represents the mean relevance of each predictor variable, whereas shaded areas represent the maximum importance of each variable. The matrix of environmental predictors was reduced beforehand to select the most representative and least collinear variables (Supporting Information Fig. S3; see the Materials and Methods section).

on the intercept. The model did not evidence any influence of the methodology used on abundance data ( $P=0.73$ ; Fig. S1a).

Further, five different methods to estimate soil algal  $\text{CO}_2$  fixation were reported in our database: biomass growth quantification (4% of the data), biological oxygen demand (BOD; 4% of the data), Chl fluorescence (4%), infrared  $\text{CO}_2$  gas analyzer (82%), and isotopic labelling ( $^{14}\text{C}$ , 6%). All these methods strictly focused on microbial photosynthetic activity (i.e.  $\text{CO}_2$  fixation in the presence of light) and minimized or avoided possible nonphototrophic  $\text{CO}_2$  fixation by subtracting dark  $\text{CO}_2$  fixation rates from light  $\text{CO}_2$  fixation rates. Though these techniques differ, they usually are in agreement and give similar trends (Peterson, 1980; Richardson *et al.*, 1984; Hamard *et al.*, 2021a). However, depending on the technique, net photosynthesis of algae can be overestimated (e.g. BOD and Chl fluorescence which provide maximal photosynthetic rates) or underestimated (e.g.  $^{14}\text{C}$  isotopic labelling; Richardson *et al.*, 1984), especially under conditions of low nutrient and/or high light (Peterson, 1980). Nevertheless, although biomass and isotopic labelling

methods tend to overestimate soil algal NPP ( $P<0.05$ ), we found that this trend was biome driven and was not significant within biomes ( $P=0.06$ ; Fig. S1b).

Unless mentioned otherwise, soil algal C flux rates from studies providing estimates on an annual basis were included without modification in the data base. Soil algal C flux values reported in micromoles, microgram, milligrams, seconds, minutes, hours, or days were converted into  $\text{g m}^{-2} \text{yr}^{-1}$ . As microbial photosynthesis neither occurs every day of the year nor all day long, we constrained the microbial photosynthetic activity to about one-third of a day (8 h), for a limited period of time during the year: 80 d in arctic areas, 150 d in subarctic areas, 240 d in temperate areas, and 300 d in tropical areas. Maximal photosynthetic rates under optimal conditions were limited to about one-third of the maximal value to account for limitations of photosynthetic activity and dark respiration (Elbert *et al.*, 2012). Reported rates that did not take into account dark respiration were scaled with a factor of two-thirds, as showed by our specific measurements in the field (Fig. S2).



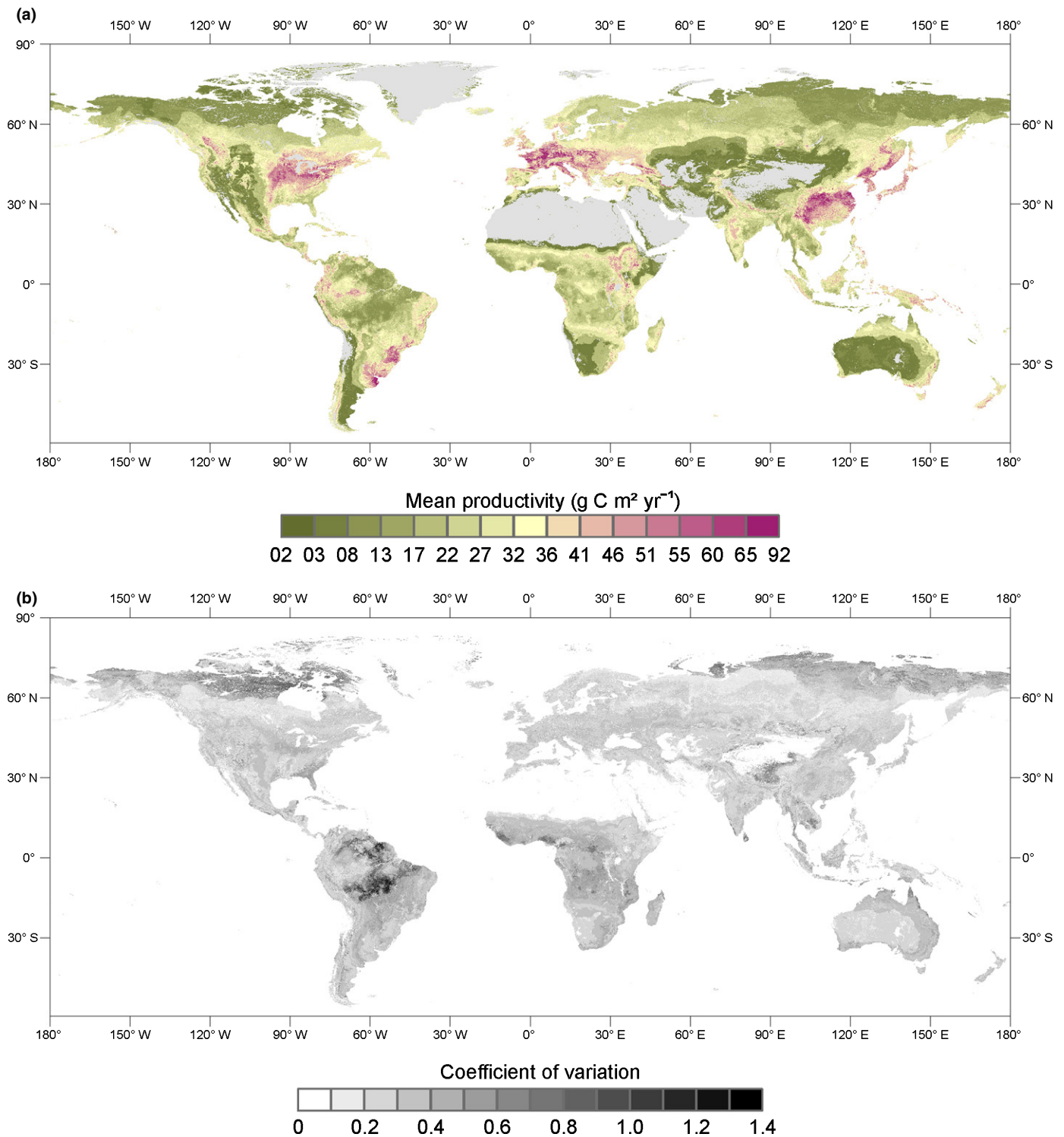


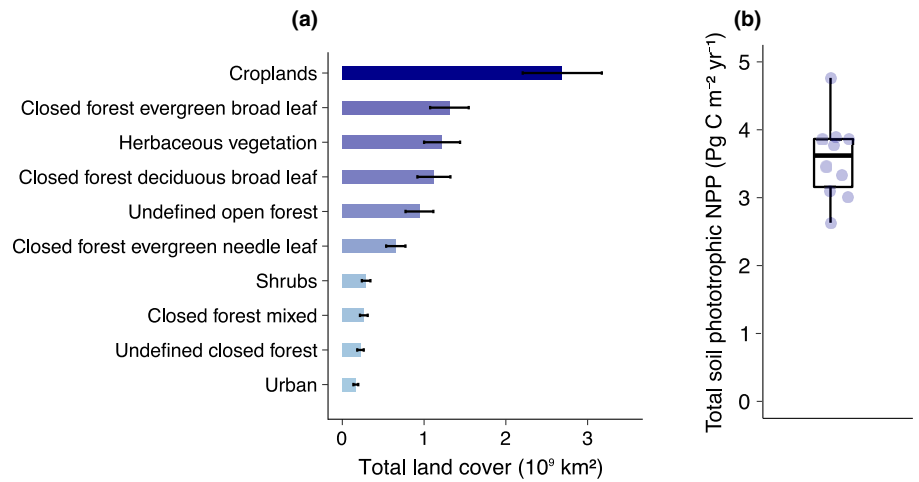
**Fig. 3** Global map of soil algal net primary productivity (NPP) at the 30 arcsec pixel scale (c. 1 km<sup>2</sup>). (a) NPP (g carbon (C) m<sup>-2</sup> yr<sup>-1</sup>) of soil algae in surface soil. Pixel values were binned into 15 quantiles to create the color palette. Grey color indicates area not investigated. (b) Coefficient of variation (SD as a fraction of the mean predicted value) as a measure of soil algal primary productivity prediction accuracy. Overall, our prediction error is low, with the exception of a low soil algal C flux rate in tropical forests and boreal zones. Pixel values were binned into 15 quantiles to create the color palette.

### Environmental data collection

In order to identify the main environmental drivers of the abundance and NPP of soil algae, and create spatial predictive models

of primary productivity, we sampled a stack of 55 environmental variables at each of the data point locations using the Google Earth Engine platform (Gorelick *et al.*, 2017) (Table S3). The stack was composed of 19 long-term climate variables extracted

**Fig. 4** Dominant land uses in soil algal net primary productivity (NPP) hotspots and total soil algal NPP. (a) The mean and SE ( $n = 10$ ) of the land uses identified in the four hotspots of soil algal NPP ( $> 50 \text{ g m}^{-2} \text{ yr}^{-1}$ ) from the 10 prediction maps (Supporting Information Fig. S7) used to build the final map presented in Fig. 3(a). (b) The median and interquartile range ( $n = 10$ ) of the total soil algal productivity per year from the 10 ensemble random forest models used in the prediction maps presented in Fig. 3(a).



from the WorldClim V1 database. They averaged monthly data spanning the period 1960–1991. An additional 14 long-term climate variables were extracted from TerraClimate and averaged for the period 1958–2019. Several vegetation related variables were extracted from Terra Moderate Resolution Imaging Spectroradiometer: vegetation indices as proxies for plant cover (leaf area index (LAI) and biomass (normalized difference vegetation index (NDVI), enhanced vegetation index (EVI)), as well as values of primary productivity (NPP, gross primary production (GPP)). We acknowledge that NDVI, EVI, LAI, NPP, and GPP are derived from remote-sensing reflectance and can thus be sensitive to the Chl fluorescence content of soil algae. However, under plant coverage, we assume that their contribution to surface reflectance remains minor compared with the plant foliage (Chen *et al.*, 2005). Seven soil variables were extracted from the OpenLand database for the 0–5 cm soil depth. Five variables on soil moisture were downloaded from the NASA-USDA Global soil moisture and the NASA-USDA Soil Moisture Active Passive Global soil moisture datasets. Elevation data were retrieved from the Global Multi-resolution Terrain Elevation Data 2010. Human population density and latitudes and longitudes were also integrated in the analyses. All details about environmental variables are given in Table S3.

Data were acquired using the Google Earth Engine platform (Gorelick *et al.*, 2017). Long-term statistics (mean, median, minimum, and maximum values) were calculated for the whole available period in each database for integration in our numerical analyses. To harmonize the different environmental layers across the globe, it was necessary to aggregate or disaggregate (when appropriate) the spatial resolution of the different layers to match a 30 arcsec resolution. Following the spatial harmonization, the global layers were matched with each of the 203 data-point locations.

#### Identification of the variables of importance in driving soil algal abundance and net primary productivity

We employed a clustering approach using the CLUSTOFVAR package (Chavent *et al.*, 2012) in R to reduce the environmental

covariates of interest and select the most representative and least collinear variables. We tested a range of cluster numbers (5, 10, 15, and 20) using CLUSTOFVAR to define the best number of variables to test in ML modelling. Fifteen variables of interest were identified using CLUSTOFVAR (see details in Fig. S3), related to climate (bio03, bio04, bio10, bio11, bio12, bio14, bio15), vegetation cover (lai), soil (moist, soc, bulk, ph, sand), and geographic (lon) conditions (abbreviations for these variables are given in Table S3 and Fig. 2). We then identified the main environmental drivers of soil algal abundance and NPP among these 15 variables using the Boruta algorithm, a wrapper of random forest (RF) and one of the most efficient tools for variable selection (Degenhardt *et al.*, 2019). The Boruta algorithm compares the importance of predictor variables with those of random so-called shadow variables using statistical testing and several runs of RFs. The Boruta algorithm was computed for the entire dataset using 1000 iterations.

#### Predicting soil algal net primary productivity by means of machine-learning modelling

Training ML models on a relatively small number of observations can lead to overfitting and produce inaccurate results. As gathering a bigger dataset to overcome these problems was impossible due to the limited number of available studies in the literature, we used a series of methods and targeted sensitive analyses testing the robustness of our predictions. Particular attention was given to the distribution of data, the number of predictors used, the choice of the model(s) and its (their) hyperparameters, cross-validation strategies, and confidence prediction intervals (Bishop, 2006; Lesmeister, 2019):

- (1) We inspected the distribution of the soil algal NPP values and searched for outliers, as they can strongly influence the model and its prediction. One extremely high and unrealistic value was removed from the database (see Table S2 for details).
- (2) We implemented our ML models with the most relevant predictors for soil algal NPP based on Boruta analysis (see earlier herein). Usually, explicit predictor selection is not the best

approach for ML, but it is an essential step when data size is limited to avoid overfitting (Meyer *et al.*, 2018).

(3) Because complex ML models with many parameters (e.g. neural networks approaches) are more prone to overfitting issues (Bishop, 2006; Lesmeister, 2019), we selected and tested six classes of relatively simple ML algorithms trained on the six best environmental variables identified with the Boruta algorithm to spatially predict soil algal NPP (see the Results and Discussion section). We considered the most common ML models, including a simple generalized linear model, an L1-regularization regression linear model, a Bayesian generalized linear model,  $k$ -nearest-neighbor, bagged multivariate adaptive regression splines, and RF as a benchmark. We further combined all ML algorithms into a stack ensemble model as predictions from more than one ML algorithm may give better predictive performance than could be obtained from any of the basic or essential learning algorithms alone (Lesmeister, 2019). These ML model types were chosen either because they were previously used for spatial predictions or because the general ML literature suggests that they could perform well for this task (Table S4). Each of the ML models included model-specific tuning parameters that were left at default values for initial testing and comparison. To assess the predictive performance of the models, we split the total number of points into a training set and a test set using an 80 : 20 random split. We used the training set to train the different models and the test set to test their performance. We evaluated the model strength using  $k$ -fold cross-validation (with  $k = 10$ ). For each  $k$ , we stored the vector of soil algal NPP predictions, which was then used to generate predictive statistics, namely the squared Pearson's correlation between observed soil algal NPP values and those predicted (noted  $R^2$ ) and the root-mean-squared error (RMSE). We found that all ML algorithms can successfully predict soil algal NPP, although RF outperformed other ML algorithms by a significant margin (Fig. S4). The ensemble model did not perform better than RF ( $P = 0.98$ , ANOVA) while giving higher RMSE (Fig. S4). As RF performs better overall and has been demonstrated to provide robust predictions for small sample sizes (Ramezan *et al.*, 2021), we selected RF to create a predictive, high-resolution map of soil algal NPP across the globe, as described later herein.

(4) We used a grid-search procedure to iteratively tune the hyperparameters of our RF model in R using the RANDOMFOREST and CARET packages (Kuhn, 2008): the number of trees to grow (ntree; 50, 150, 250, 350, or 450) and the number of variables sampled at each split (mtry; 2–6), resulting in a total of 25 RF models. The values ntree = 350 and mtry = 4 were defined as the best hyperparameters. We used the training set to determine the best set of model hyperparameters, and to train the model. We used the test set to assess out-of-sample error, as well as model prediction performance using  $R^2$  and RMSE values, as explained earlier.

(5) We used four strategies to cross-validate our best RF model and generate statistics of the model robustness and predictive power (Fig. S5). The first strategy focused on the size of the dataset and corresponded to a common  $k$ -fold cross-validation where observations were randomly split into  $k$  sets of decreasing size (hereafter,  $k$ -fold 'size CV') ignoring any structure of potential spatial dependence in the data. Model training was then

performed iteratively on  $k - 1$  sets. Here, we used  $k = 6$ ; we iteratively and randomly selected 100%, 90%, 80%, 70%, 60%, and 50% of the dataset to train our RF models. We chose to maintain the integrity of our dataset and not remove a subset of data at the beginning as it would mean the loss of geographic representation. As a test set, we used a dataset in which only unique pairs of coordinates were present (65 pairs in total instead of 102 data points; hereafter 'paired dataset'). We summarized our initial dataset using the median applied on similar pairs of coordinates. As local variability could reach  $150 \text{ g C m}^{-2} \text{ yr}^{-1}$ , this approach enabled us to obtain a validation dataset for accuracy assessment. The second strategy (i.e. the  $k$ -fold 'shuffled CV') is inspired by 'null-model' analyses in ecology and tests the assumption that our predictions are not random and driven by our environmental predictors. To do so, we randomized the environmental predictors matrix to break any structure of environmental dependence in the data. We iteratively and randomly shuffled the environmental matrix 10 times ( $k = 10$ ) before training our RF models. The third strategy (i.e.  $k$ -fold 'spatial CV') differs from the size CV in that observations are split into spatially structured clusters (Ploton *et al.*, 2020). Here, the objective was to group observations into spatial clusters and take into consideration the variability generated by the multiple measurements at the same locations, or nearby, in our dataset. Spatial clusters were generated using a hierarchical cluster analysis (Ward's hierarchical agglomerative linkage method) of the distance matrix of coordinates and a clustering height of  $H = 50 \text{ km}$ . Here, we used  $k = 10$ ; we iteratively and randomly selected data within each spatial cluster to train our RF models. The maximum size of the  $k$ -datasets was 65; that is, the maximum number of unique pairs of coordinates in our paired dataset. Here again, the paired dataset was used as a test set. The fourth strategy ( $k$ -fold 'predictor variable shuffling (PVS) CV') tests the assumption that our model gets overfitted by the covariance among environmental predictors. To refute this assumption, we randomly shuffled the values of one, two, three, four, and five predictors before training the RF model. PVS CV was run on spatially clustered training sets (same approach as spatial CV) with  $k = 100$  to cover all random combinations among predictors. For each CV strategy, we stored the vector of soil algal NPP predictions, which was then used to generate CV statistics, namely  $R^2$  and the RMSE.

(6) To assess any further overfitting and/or highly optimistic evaluations of the predictive power of our RF model due to the spatial dependence in the raw data and model residuals (Ploton *et al.*, 2020), we tested for spatial autocorrelation in the raw data and in the size and spatial CV model residuals (Fig. S6). We observed spatial autocorrelation using empirical variograms and did not evidence any particular spatial autocorrelation. The geostatistical analysis GSTAT R package (Pebesma & Heuvelink, 2016) was used for variogram and spatial autocorrelation testing.

(7) Like many algorithmic approaches to prediction, RF typically produces point predictions that are not accompanied by information about how far those predictions may be from true response values. To cross-validate and quantify this issue, we used prediction intervals that estimate the interval into which future observations will fall with a given probability (Meinshausen,

2006). In other words, it calculates the confidence or certainty in the prediction. We used 'out-of-the bag' (OOB) prediction intervals as a straightforward approach for constructing our RF prediction intervals (Zhang *et al.*, 2020). As described for the spatial CV strategy, we generated 10 independent subsets of our entire dataset, stratified by spatial clusters. For each independent subset, we trained our best RF and calculated OOB prediction intervals at each run. Then, we classified whether data points from the test dataset fell within or outside RF prediction intervals.

All comparative and cross-validation analyses were performed in R (R Core Team, 2019).

### Mapping soil algal net primary productivity and evaluating model uncertainties

To create the final map of soil algal NPP and represent the confidence in our estimates for each pixel, we used an ensemble approach (van den Hoogen *et al.*, 2019; Ma *et al.*, 2021). We averaged the global predictions from 10 RF models trained on 10 independent subsets of our entire dataset, stratified by spatial clusters to proportionally represent the major bioclimatic zones in each of the 10 independent subsets (spatial CV strategy). This approach minimizes the influence of any single prediction, thereby stabilizing variation and minimizing bias that can otherwise arise from extrapolation or in-fit overfitting when using a single ML model (Sagi & Rokach, 2018). The 10 independent RF models were run with the six best environmental variables identified through the Boruta algorithm and using the best-performing set of hyperparameters (Fig. S7). Through this approach, we thus returned the best RF model 10 times using 10 different training sets that took into account local variability. We then used the mean predicted value across the 10 RF models as the final prediction of soil algal NPP for each pixel. Finally, from these 10 models, we further calculated per-pixel coefficient-of-variation values (SD divided by the mean predicted value) as a measure of prediction uncertainty (Ma *et al.*, 2021). In addition, we assessed the extent of extrapolation in our models; that is, how well our sampled data spread throughout the full environmental space, following van den Hoogen *et al.* (2019). In particular, we examined how many of the Earth's pixels existed outside the range of our sampled data for each of the six environmental layers used in our RF model. To do so, we extracted the minimum and maximum values of each environmental layer of the pixels in which our sampling sites were located. Then, for each environmental layer, we evaluated the number of terrestrial pixels that fell outside the sampled range and calculated the relative proportion of interpolation; that is, the percentage of environmental bands that fell into the sampled range. Next, we created a per-pixel representation of the relative proportion of interpolation and extrapolation (Fig. S8). All geospatial and extrapolation analyses were performed in Google Earth Engine (Gorelick *et al.*, 2017).

### Cross-validation map of soil algal net primary productivity

As an additional validation exercise, we estimated annual soil algal NPP following the biome-based land cover approach taken

by Elbert *et al.* (2012). Soil algal NPP was estimated by multiplying the global ground area surface of a particular biome with its corresponding median of algal C uptake flux (Fig. 1). Biome land covers were recovered from the Global Land Cover Characterization database v.2.0 (<https://www.usgs.gov/centers/eros/science/usgs-eros-archive-land-cover-products-global-land-cover-characterization-glcc>) and reclassified according to our biome classes: grasslands, drylands, broadleaf and mixed forests, alpine and polar lands, wetlands, croplands, and broadleaf evergreen forests.

## Results and Discussion

### Biome-level patterns of soil algal density and net primary productivity

By compiling a dataset on microscopic abundance observations ( $n = 115$ ; Table S1), we found on average  $(5.5 \pm 3.4) \times 10^6$  soil algae per g of dry topsoil (Fig. 1b). Soil algal density varied within and across biomes, ranging from thousands to millions of individuals per g of dry soil (Fig. 1c). Overall, soil algal abundances ( $10^5$  cells per g of dry soil) were highest in wetlands (median = 1036), grasslands (median = 410), broadleaf evergreen forests (median = 202), and croplands (median = 161), whereas the lowest densities were found in drylands (median = 85), broadleaf and mixed forests (median = 59), and alpine and polar lands (median = 20) (Fig. 1c). These findings show discrepancies with the most recent assessments of the biogeographic distribution of soil algae based on DNA sequencing approaches (Cano-Díaz *et al.*, 2020; Oliverio *et al.*, 2020). These previous studies suggest that soil algae are typically abundant in arid soils, encompassing up to 40% of the total eukaryotic community (Oliverio *et al.*, 2020) and 4% of the total prokaryotic community (Cano-Díaz *et al.*, 2020). However, even though data based on amplicon gene sequencing give arguably an accurate picture of microbial diversity, our findings illustrate that they cannot be used to infer biogeographic patterns of algal density in soils. Nevertheless, DNA sequencing data could explain the patterns of absolute abundance seen in this study (Hamard *et al.*, 2021a). The blooming of specific taxa resulting from taxonomic turnover in response to specific soil conditions could drastically increase total soil algal abundance (Karaoz *et al.*, 2018).

To identify the main environmental variables that drive algal density in soils, we related the density of soil algae to environmental factors. In contrast to soil invertebrates (van den Hoogen *et al.*, 2019) and total microbial biomass (Xu *et al.*, 2013), our analysis did not reveal notable latitudinal and/or longitudinal effects on soil algal abundance. Instead, and as shown for the community composition of micro-eukaryotes (Oliverio *et al.*, 2020; Aslani *et al.*, 2021) and bacteria (Delgado Baquerizo *et al.*, 2018), we found that climate (i.e. temperature and precipitation) was a main driver of the global distribution of total algal density in soils. However, plant cover (i.e. LAI) and soil characteristics (i.e. soil moisture, soil organic C content, and pH) were as important as climate (Fig. 2a). In particular, mean annual temperature and precipitation, vegetation cover, and soil moisture



had strong positive effects, whereas increasing pH had a negative effect on total soil algal abundance (Fig. S9). Although the exact mechanisms behind these interactions still need to be identified, our results indicate that complex interactions among soil properties, climate, and vegetation determine the growth efficiency of soil algae. Our findings suggest that frequent rainfall and plant cover facilitate the size distribution and connectedness of aqueous microbial habitats in soils by increasing water retention in soil pores. This, in turn, promotes microbial cell motility, cell-to-cell interactions (Bickel & Or, 2020), and, therefore, algal abundance in topsoils. In contrast to the general assumption that arid environments are the main habitat for soil algae (Oliverio *et al.*, 2020), we show here that soil algae are widespread and more abundant in absolute numbers in acidic, wet, and vegetated areas. These results further suggest that the contribution of soil algae to terrestrial productivity is particularly important in these areas.

We tested this assumption by collating a second dataset from the literature on algal NPP in surface soil, and spanning similar biomes as for the abundance data ( $n=102$ ; Fig. 1a; Table S2). On average, soil algae were responsible for a mean annual NPP of  $30 \text{ g C m}^{-2}$  ( $0.06\text{--}253.3 \text{ g C m}^{-2} \text{ yr}^{-1}$ ) across biomes (Fig. 1b). When comparing these data with terrestrial NPP at the same locations, soil algal NPP accounted for *c.* 10.3% (0.3–80%) of terrestrial NPP (Fig. 1b,c), which is consistent with the value reported by Hamard *et al.* (2021a) for peatlands (*c.* 9.3%). We found the highest algal NPP in croplands (median =  $157 \text{ g C m}^{-2} \text{ yr}^{-1}$ ), broadleaf and mixed forests (median =  $28.2 \text{ g C m}^{-2} \text{ yr}^{-1}$ ), grasslands (median =  $22.6 \text{ g C m}^{-2} \text{ yr}^{-1}$ ), and broadleaf evergreen forests (median =  $18 \text{ g C m}^{-2} \text{ yr}^{-1}$ ) (Fig. 1c), supporting our empirical and independent observations on absolute abundance (Fig. 1c). We further showed that the absolute abundance and NPP of soil algae were largely driven by the same environmental variables (Fig. 2), especially soil moisture, vegetation cover, and annual precipitation (Fig. S9). The positive correlation between soil algal NPP and increasing vegetation cover might be seen as counterintuitive given that plant canopy reduces the light availability at the soil surface. However, most microscopic algae show optimal photosynthesis at low light intensity (Ritchie & Larkum, 2012; Hamard *et al.*, 2021a) by optimizing light harvesting at low light flux (Perrine *et al.*, 2012). Given the positive relationship between total microbial abundance and metabolic rates in soils (Johnston & Sibly, 2018), our results further presume a simultaneous increase in soil algal abundance and productivity with increasing environmental favorability, which corroborates previous findings in aquatic systems (Y. Liang *et al.*, 2017).

### Global biogeography of soil algal net primary productivity

We implemented an ensemble of 10 RF models (Fig. S7) to predict soil algal NPP based on the six best covariate layers (Fig. 2); that is, annual precipitation, soil moisture, vegetation cover, soil organic C content, vapor pressure deficit, and soil sand content (see the Materials and Methods section). Our ensemble RF models predicted the test data reasonably well (averaged  $R^2=0.51$ ,  $\text{RMSE}=0.84$ , or  $2.4 \text{ g C m}^{-2} \text{ yr}^{-1}$ ; Fig. S10). It showed a fairly

linear relationship with observed soil algal NPP, although predicted NPP tended to be overestimated at low NPP and underestimated at high NPP – a common bias pattern resulting from the RF algorithm (Xu *et al.*, 2016). Nevertheless, a sensitivity analysis based on RF prediction intervals showed that nearly 93% of observations from the test dataset fell within the RF prediction intervals (Fig. S11). This indicates that our RF model provides unbiased results, with predictions falling within the full range of observed data. Further rigorous *k*-fold cross-validation steps (Fig. S5) revealed that RF predictions did not lead to overfitting by the possible covariance among predictors (Fig. S12) and were robust without issues due to the size of the data set (size CV:  $R^2=0.47$  and  $\text{RMSE}=0.98$ ; Figs S13, S14), the spatial structure of the data (spatial CV:  $R^2=0.39$  and  $\text{RMSE}=1.04$ ; Fig. S13), or possible stochasticity in the predictions (shuffled CV:  $R^2=0.02$  and  $\text{RMSE}=1.4$ ; Fig. S13). Our cross-validation hence indicates that soil algal NPP can be reasonably predicted while providing accurate predictions within confidence intervals and avoiding overfitting. We therefore used our spatially unbiased RF models (spatial CV approach) to upscale observed soil algal NPP across the globe and to map the global distribution of soil algal NPP (Fig. 3).

The quantitative map of soil algal net C fixation showed fixation rates ranging between  $2.3 \pm 0.3$  and  $84 \pm 32.4 \text{ g C m}^{-2} \text{ yr}^{-1}$  (Fig. 3a). Overall, the predictive uncertainty was relatively low, although areas of substantial uncertainty still remain in tropical (central Brazil) and subarctic (north Canada) regions (Fig. 3b). Despite these uncertainties, the map produced through RF modelling provided a more detailed and accurate spatial distribution of soil algal NPP than the low-resolution map extrapolated from biome land-cover (Fig. S15). The map did not reveal notable latitudinal trends, unlike other soil C processes, such as soil respiration (Xu *et al.*, 2013), bacterial and fungal biomass (He *et al.*, 2020), and microbial residence time (He & Xu, 2021). However, it highlighted four hotspots of soil algal NPP ( $> 50 \text{ g C m}^{-2} \text{ yr}^{-1}$ ), in northeastern North America, southeastern South America, central and western Europe, and eastern Asia (Fig. 3a). Further analysis of land cover showed that these four hotspots are dominated by croplands and forests (Fig. 4a), which is in good concordance with our empirical observations (Fig. 1c).

Globally integrated, soil algal NPP amounted to *c.*  $3.6 \text{ Pg C yr}^{-1}$  ( $2.6\text{--}4.8 \text{ Pg C yr}^{-1}$ ; Fig. 4b), which is slightly higher than the value reported for soil cryptogams, and that includes bryophytes and lichens ( $0.34\text{--}3.3 \text{ Pg C yr}^{-1}$ ; Elbert *et al.*, 2012; Porada *et al.*, 2013). A few factors may be responsible for this counterintuitive difference. First, our estimation did not focus on cryptogams ground cover only (Elbert *et al.*, 2012) but on the whole ground surface. Second, our data compilation on soil algal NPP much exceeds previous efforts and not only included drylands but also many wetter areas, such as croplands, rainforests, and wetlands. These regions evidenced algal NPP values two to eight times higher than in drylands (Fig. 1c), on which previous estimations are mostly based (Elbert *et al.*, 2012; Rodriguez-Caballero *et al.*, 2018). Third, previous estimates mostly included cyanobacterial NPP (Elbert *et al.*, 2012). Many cyanobacteria are facultative heterotrophs and often downregulate their own

photosynthesis to nearly 10% of their maximum rate when cooccurring with plants, as they get C from them (Adams & Duggan, 2008).

### General implications

With nearly 3.6 Pg C taken up annually, soil algae contribute to *c.* 6.4% of the global terrestrial NPP (*c.* 56 Pg C yr<sup>-1</sup>; Zhao *et al.*, 2005) – again supporting our independent empirical observations across biomes (Fig. 1b). Such a contribution to terrestrial NPP might seem relatively high considering the low C biomass of soil algae compared with terrestrial plant biomass (Bar-On *et al.*, 2018). Yet, the photosynthetic capacity of soil algae is comparable to plants when considering their Chl content per unit area (Fig. S16; Table S5). Furthermore, the small fraction of C found in live standing biomass of soil algae does not reflect the amount of C cycled through this pathway, as microbial growth rates and turnover are much higher than in plants. Accordingly, one might argue that most of the C fixed by soil algae is then rapidly released through respiration and decomposition as soil algae die, minimizing their impact on soil C sequestration. However, recent findings showed that C in soil algal biomass (Yuan *et al.*, 2012) and microbial necromass (Liang *et al.*, 2019) can significantly contribute to soil organic C, thus suggesting that soil algae play a role in soil C sequestration in the long term. Nevertheless, this contribution to soil C sequestration most probably depends on multifactorial environmental factors (Liang *et al.*, 2019), as well as on the formation and mean residence time of soil algal-derived organic products (Hu *et al.*, 2020). Furthermore, soil algal activity may also initiate hotspots and hot moments of heterotrophic activity in soils by providing resource subsidies to heterotrophic (micro)organisms, either as food for consumers – such as heterotrophic micro-eukaryotes (Seppey *et al.*, 2017), earthworms, and springtails (Schmidt *et al.*, 2016) – or through the release of labile C that could prime heterotrophic activity (Wyatt & Turetsky, 2015), and hence stimulate decomposition processes in soils (Wyatt & Turetsky, 2015; Halvorson *et al.*, 2019). Although the influence of soil algae in terms of C sequestration and release still remains virtually unknown, our findings indicate that they are important players in global soil C uptake, and hence should be taken into account in terrestrial C models.

Despite the confidence in our estimates, we caution that some bias might affect the exact numbers of predicted annual soil algal NPP. First, most algal productivity data rely on snapshot measurements, as continuous, high-resolution measurements of algal NPP in soils are scarce. We thus used some assumptions to estimate annual soil algal NPP (see Table S2 and the Materials and Methods section) and acknowledge that seasonal variation in algal photosynthetic activity due to differences in climatic conditions, light, and nutrient availability may influence our estimations. Second, though our model predictions reflects well the observed variation in soil algal NPP across large spatial gradients (e.g. biomes), we acknowledge there are still some limits regarding our ability to accurately predict at smaller spatial scales. Soil algal diversity and community composition (Hamard *et al.*, 2021a,b), predation strength (Schmidt *et al.*, 2016), and/or soil

nutrient availability (Gilbert *et al.*, 1998) can influence soil algal activity at small spatial scales. Therefore, some of the unexplained variation in our RF model is probably due to missing plot-level information where soil algal NPP was quantified, explaining the lower range in our RF predictions compared with observations. We minimized this issue by including data from close locations as much as possible. In addition, our spatial CV taking into account local variability did not show a sharp decline in model  $R^2$ , suggesting that local variation does not substantially affect the numbers obtained. Finally, we further note that the size of our dataset is limited, as in all other global studies on soil biodiversity (Delgado Baquerizo *et al.*, 2018; van den Hoogen *et al.*, 2019; Cano-Díaz *et al.*, 2020; Oliverio *et al.*, 2020), with some regions being underrepresented. Although our data compilation exceeds previous efforts, and even if we attempted to minimize all issues regarding overfitting and the size of our dataset, the risk that our estimations deviate from the true mean remains, particularly in areas with low sampling density (Fig. 3b). Nevertheless, we tested the extent of extrapolation of our RF model by examining how many of the Earth's pixels existed outside the sampled range of our environmental covariates used in the RF model (see the Materials and Methods section). We found that our samples covered the vast majority of environmental conditions on Earth, with 88% of Earth's pixels having at least > 80% of the predictor bands falling within the sampled range of environmental conditions (Fig. S8), thus providing confidence in our estimations.

In conclusion, our synthesis presents the most comprehensive assessment of the distribution of soil algae and the global importance of microbial photosynthesis in soil C uptake. Our findings alter some of our most basic assumptions about the role of microorganisms in soil ecological functions by showing that microbial photosynthesis is not only a major component in aquatic ecosystems but also in most terrestrial biomes. We cautiously conclude that soil algae add a so far not considered additional 3.6 Pg C yr<sup>-1</sup> to net terrestrial C uptake, which is equivalent to *c.* 31% of the global anthropogenic C emissions (*c.* 11.5 ± 0.9 Pg C; Friedlingstein *et al.*, 2019). Although our estimate of total soil algal NPP will undoubtedly be refined with future data collection, our findings indicate that soil algae are, together with nonphotosynthetic microbial CO<sub>2</sub> fixation (Spohn *et al.*, 2019; Akinyede *et al.*, 2020), major players in the global soil C balance. Preserving the unseen soil (algal) biodiversity locally and across biomes has never been more important as the urgency to harness all available opportunities to reduce atmospheric CO<sub>2</sub> grows.

### Acknowledgements





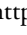
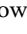


We acknowledge the work of all researchers that collected these data over the years. This research has been supported by MIXOPEAT, a project funded by the French National Research Agency (grant no. ANR-17-CE01-0007) to VEJJ. VEJJ and RW acknowledge financial support from the French National Research Agency through an Investissement d'Avenir (Labex CEBA, ref. ANR-10-LABX-25-01). ML was funded by a grant from the National Science Centre (Poland) (no. 2015/17/B/

ST10/01656). TH acknowledges support from HES-SO (project 78046, MaLDiveS) and the Swiss Federal Office for the Environment (19.0061.PJ.PZ/D-91173401/988, MiDiBo\_2). PK acknowledges financial support from the Swedish Research Council Formas (2017-00366). EL wishes to acknowledge the program 'Atracción de Talento Investigador' from the Consejería de Educación, Juventud y Deporte, Comunidad de Madrid, Spain (2017-T1/AMB-5210) and the project MYXOTROPIC funded by the Spanish Government PGC2018-094660-B-I00 (MCIU/AEI/FEDER,UE) for financial support. We thank A. Austin and the three anonymous reviewers for their helpful and constructive comments on our manuscript.

## Author contributions

VEJJ developed the study designed with the help of EL, PK, ML, and TH. VEJJ and TH performed the literature review. VEJJ collected the data with the contribution of ML, EL, TH, SG and SH. VEJJ and RW gathered and organized the data. RW collected the environmental and land cover data. VEJJ performed all ML analyses. RW mapped soil algal productivity with the help of VEJJ. SH performed additional photosynthesis and Chl biomass analyses on soil algae. VEJJ carried out statistical analyses and created the figures. VEJJ and EL wrote the first draft of the manuscript with inputs from PK, SG and RW. All authors discussed the results and commented on the manuscript.

## ORCID

Stefan Geisen  <https://orcid.org/0000-0003-0734-727X>  
 Samuel Hamard  <https://orcid.org/0000-0002-9811-4131>  
 Thierry Heger  <https://orcid.org/0000-0003-3614-0964>  
 Vincent E. J. Jassey  <https://orcid.org/0000-0002-1450-2437>  
 Paul Kardol  <https://orcid.org/0000-0001-7065-3435>  
 Mariusz Lamentowicz  <https://orcid.org/0000-0003-0429-1530>  
 Enrique Lara  <https://orcid.org/0000-0001-8500-522X>  
 Romain Walcker  <https://orcid.org/0000-0002-5769-810X>

## Data availability

All environmental covariates are available online (see Table S3 for details). All data needed to evaluate the conclusions in the paper are present in the paper and/or the Supporting Information. Data and codes related to this paper are available from Figshare (10.6084/m9.figshare.c.5136497).

## References

- Adams DG, Duggan PS. 2008. Cyanobacteria–bryophyte symbioses. *Journal of Experimental Botany* 59: 1047–1058.
- Akinyede R, Taubert M, Schruppf M, Trumbore S, Küsel K. 2020. Rates of dark CO<sub>2</sub> fixation are driven by microbial biomass in a temperate forest soil. *Soil Biology and Biochemistry* 150: e107950.
- Amelung W, Bossio D, de Vries W, Kögel-Knabner I, Lehmann J, Amundson R, Bol R, Collins C, Lal R, Leifeld J *et al.* 2020. Towards a global-scale soil climate mitigation strategy. *Nature Communications* 11: e5427.
- Aslani F, Geisen S, Ning D, Tedersoo L, Bahram M. 2021. Towards revealing the global diversity and community assembly of soil eukaryotes. *Ecology Letters* 25: 65–76.
- Bar-On YM, Phillips R, Milo R. 2018. The biomass distribution on Earth. *Proceedings of the National Academy of Sciences, USA* 115: 6506–6511.
- Bay SK, Dong X, Bradley JA, Leung PM, Grinter R, Jirapanjawan T, Arndt SK, Cook PLM, LaRowe DE, Nauer PA *et al.* 2021. Trace gas oxidizers are widespread and active members of soil microbial communities. *Nature Microbiology* 6: 246–256.
- Beal J, Farny NG, Haddock-Angelli T, Selvarajah V, Baldwin GS, Buckley-Taylor R, Gershtater M, Kiga D, Marken J, Sanchania V *et al.* 2020. Robust estimation of bacterial cell count from optical density. *Communications Biology* 3: e512.
- Bickel S, Or D. 2020. Soil bacterial diversity mediated by microscale aqueous-phase processes across biomes. *Nature Communications* 11: 116–119.
- Bishop CM. 2006. *Pattern recognition and machine learning*. Information Science and Statistics Series. New York, NY, USA: Springer.
- Brostoff WN, Rasoul Sharifi M, Rundel PW. 2005. Photosynthesis of cryptobiotic soil crusts in a seasonally inundated system of pans and dunes in the western Mojave Desert, CA: field studies. *Flora – Morphology, Distribution, Functional Ecology of Plants* 200: 592–600.
- Cano-Diaz C, Maestre FT, Eldridge DJ, Singh BK, Bardgett RD, Fierer N, Delgado-Baquerizo M. 2020. Contrasting environmental preferences of photosynthetic and non-photosynthetic soil cyanobacteria across the globe. *Global Ecology and Biogeography* 29: 2025–2038.
- Chavent M, Simonet VK, Liquet B, Saracco J. 2012. CLUSTOFVAR: an R package for the clustering of variables. *Journal of Statistical Software* 50: 1–16.
- Chen J, Zhang MY, Wang L, Shimazaki H, Tamura M. 2005. A new index for mapping lichen-dominated biological soil crusts in desert areas. *Remote Sensing of Environment* 96: 165–175.
- Crowther TW, van den Hoogen J, Wan J, Mayes MA, Keiser AD, Mo L, Averill C, Maynard DS. 2019. The global soil community and its influence on biogeochemistry. *Science* 365: eaav0550.
- Degenhardt F, Seifert S, Szymczak S. 2019. Evaluation of variable selection methods for random forests and omics data sets. *Briefings in Bioinformatics* 20: 492–503.
- Delgado-Baquerizo M, Oliverio AM, Brewer TE, Benavent-González A, Eldridge DJ, Bardgett RD, Maestre FT, Singh BK, Fierer N. 2018. A global atlas of the dominant bacteria found in soil. *Science* 359: 320–325.
- Dettweiler-Robinson E, Nuñez M, Litvak ME. 2018. Biocrust contribution to ecosystem carbon fluxes varies along an elevational gradient. *Ecosphere* 9: e02315.
- Elbert W, Weber B, Burrows S, Steinkamp J, Büdel B, Andreae MO, Pöschl U. 2012. Contribution of cryptogamic covers to the global cycles of carbon and nitrogen. *Nature Geoscience* 5: 459–462.
- Field CB, Behrenfeld MJ, Randerson JT, Falkowski P. 1998. Primary production of the biosphere: integrating terrestrial and oceanic components. *Science* 281: 237–240.
- Friedlandstein P, Jones MW, O'Sullivan M, Andrew RM, Hauck J, Peters GP, Peters W, Pongratz J, Sitch S, Le Quéré C *et al.* 2019. Global carbon budget 2019. *Earth System Science Data* 11: 1783–1838.
- Ge T, Wu X, Liu Q, Zhu Z, Yuan H, Wang W, Whiteley AS, Wu J. 2016. Effect of simulated tillage on microbial autotrophic CO<sub>2</sub> fixation in paddy and upland soils. *Scientific Reports* 6: e19784.
- Gilbert D, Amblard C, Bourdier G, Francez A. 1998. The microbial loop at the surface of a peatland: structure function, and impact of nutrient input. *Microbial Ecology* 35: 83–93.
- Gorelick N, Hancher M, Dixon M, Ilyushchenko S, Thau D, Moore R. 2017. Google Earth Engine: planetary-scale geospatial analysis for everyone. *Remote Sensing of Environment* 202: 18–27.
- Halvorson HM, Barry JR, Lodato MB, Findlay RH, Francoeur SN, Kuehn KA. 2019. Periphytic algae decouple fungal activity from leaf litter decomposition via negative priming. *Functional Ecology* 33: 188–201.
- Hamard S, Céréghino R, Barret M, Sytiuk A, Lara E, Dorrepaal E, Kardol P, Küttim M, Lamentowicz M, Leflaive J *et al.* 2021a. Contribution of microbial photosynthesis to peatland carbon uptake along a latitudinal gradient. *Journal of Ecology* 109: 1365–2745.



- Hamard S, Küttim M, Céréghino R, Jassey VEJ. 2021b. Peatland microhabitat heterogeneity drives phototrophic microbes distribution and photosynthetic activity. *Environmental Microbiology* 23: 6811–6827.
- He L, Mazza Rodrigues JL, Soudzilovskaia NA, Barceló M, Olsson PA, Song C, Tedersoo L, Yuan F, Yuan F, Lipson DA *et al.* 2020. Global biogeography of fungal and bacterial biomass carbon in topsoil. *Soil Biology and Biochemistry* 151: e108024.
- He L, Xu X. 2021. Mapping soil microbial residence time at the global scale. *Global Change Biology* 27: 6484–6497.
- van den Hoogen J, Geisen S, Routh D, Ferris H, Traunspurger W, Wardle DA, de Goede RGM, Adams BJ, Ahmad W, Andriuzzi WS *et al.* 2019. Soil nematode abundance and functional group composition at a global scale. *Nature* 572: 194–198.
- Hu Y, Zheng Q, Noll L, Zhang S, Wanek W. 2020. Direct measurement of the *in situ* decomposition of microbial-derived soil organic matter. *Soil Biology and Biochemistry* 141: e107660.
- Jassey VEJ, Chiapusio G, Binet P, Buttler A, Laggoun-Défarge F, Delarue F, Bernard N, Mitchell EAD, Toussaint M-L, Francez A-J *et al.* 2013. Above and belowground linkages in *Sphagnum* peatland: climate warming affects plant–microbial interactions. *Global Change Biology* 19: 811–823.
- Johnston ASA, Sibly RM. 2018. The influence of soil communities on the temperature sensitivity of soil respiration. *Nature Ecology & Evolution* 2: 1597–1602.
- Kallmeyer J, Smith DC, Spivack AJ, D'Hondt S. 2008. New cell extraction procedure applied to deep subsurface sediments. *Limnology and Oceanography: Methods* 6: 236–245.
- Karaoz U, Couradeau E, da Rocha UN, Lim H-C, Northen T, Garcia-Pichel F, Brodie EL, Bailey MJ. 2018. Large blooms of Bacillales (Firmicutes) underlie the response to wetting of cyanobacterial biofilms at various stages of maturity. *mBio* 9: e01366-16.
- Kuhn M. 2008. Building predictive models in R using the CARET package. *Journal of Statistical Software* 28: 1–26.
- Lesmeister C. 2019. *Mastering machine learning with R: advanced machine learning techniques for building smart applications with R 3.5, 3<sup>rd</sup> edn.* Birmingham, UK: Packt Publishing.
- Liang C, Amelung W, Lehmann J, Kästner M. 2019. Quantitative assessment of microbial necromass contribution to soil organic matter. *Global Change Biology* 25: 3578–3590.
- Liang C, Schimel JP, Jastrow JD. 2017. The importance of anabolism in microbial control over soil carbon storage. *Nature Microbiology* 2: 17105–17106.
- Liang Y, Zhang Y, Wang N, Luo T, Zhang Y, Rivkin RB. 2017. Estimating primary production of picophytoplankton using the carbon-based ocean productivity model: a preliminary study. *Frontiers in Microbiology* 8: e1926.
- Ma H, Mo L, Crowther TW, Maynard DS, van den Hoogen J, Stocker BD, Terrer C, Zohner CM. 2021. The global distribution and environmental drivers of aboveground versus belowground plant biomass. *Nature Ecology and Evolution* 5: 1110–1122.
- Maier S, Tamm A, Wu D, Caesar J, Grube M, Weber B. 2018. Photoautotrophic organisms control microbial abundance, diversity, and physiology in different types of biological soil crusts. *The ISME Journal* 12: 1032–1046.
- Maron PA, Schimann H, Ranjard L, Brothier E, Domenach AM, Lensi R, Nazaret S. 2006. Evaluation of quantitative and qualitative recovery of bacterial communities from different soil types by density gradient centrifugation. *European Journal of Soil Biology* 42: 65–73.
- Meinshausen N. 2006. Quantile regression for left-truncated semicompeting risks data. *Journal of Machine Learning Research* 7: 983–999.
- Meyer H, Reudenbach C, Hengl T, Katurji M, Nauss T. 2018. Improving performance of spatio-temporal machine learning models using forward feature selection and target-oriented validation. *Environmental Modelling & Software* 101: 1–9.
- Miltner A, Kopinke F-D, Kindler R, Selesi D, Hartmann A, Kästner M. 2005. Non-phototrophic CO<sub>2</sub> fixation by soil microorganisms. *Plant and Soil* 269: 193–203.
- Miltner A, Richnow H-H, Kopinke F-D, Kästner M. 2004. Assimilation of CO<sub>2</sub> by soil microorganisms and transformation into soil organic matter. *Organic Geochemistry* 35: 1015–1024.
- Mitchell EAD, Gilbert D, Buttler A, Amblard C, Grosvernier P, Gobat JM. 2003. Structure of microbial communities in *Sphagnum* peatlands and effect of atmospheric carbon dioxide enrichment. *Microbial Ecology* 46: 187–199.
- Oliverio AM, Geisen S, Delgado-Baquerizo M, Maestre FT, Turner BL, Fierer N. 2020. The global-scale distributions of soil protists and their contributions to belowground systems. *Science Advances* 6: eaax8787.
- Pebesma E, Heuvelink G. 2016. Spatio-temporal interpolation using GSTAT. *The R Journal* 8: 204–218.
- Perrine Z, Negi S, Sayre RT. 2012. Optimization of photosynthetic light energy utilization by microalgae. *Algal Research* 1: 134–142.
- Peterson BJ. 1980. Aquatic primary productivity and the <sup>14</sup>C-CO<sub>2</sub> method: a history of the productivity problem. *Annual Review of Ecology and Systematics* 11: 359–385.
- Ploton P, Mortier F, Réjou-Méchain M, Barbier N, Picard N, Rossi V, Dormann C, Cornu G, Viennois G, Bayol N *et al.* 2020. Spatial validation reveals poor predictive performance of large-scale ecological mapping models. *Nature Communications* 11: e4540.
- Porada P, Weber B, Elbert W, Pöschl U, Kleidon A. 2013. Estimating global carbon uptake by lichens and bryophytes with a process-based model. *Biogeosciences* 10: 6989–7033.
- R Core Team. 2019. *R: a language and environment for statistical computing.* Vienna, Austria: R Foundation for Statistical Computing.
- Ramezan CA, Warner TA, Maxwell AE, Price BS. 2021. Effects of training set size on supervised machine-learning land-cover classification of large-area high-resolution remotely sensed data. *Remote Sensing* 13: e368.
- Richardson K, Samuelsson G, Hällgren JE. 1984. The relationship between photosynthesis measured by <sup>14</sup>C incorporation and by uptake of inorganic carbon in unicellular algae. *Journal of Experimental Marine Biology and Ecology* 81: 241–250.
- Ritchie RJ, Larkum AWD. 2012. Modelling photosynthesis in shallow algal production ponds. *Photosynthetica* 50: 481–500.
- Rodríguez-Caballero E, Belnap J, Büdel B, Cruzten PJ, Andreae MO, Pöschl U, Weber B. 2018. Dryland photoautotrophic soil surface communities endangered by global change. *Nature Geoscience* 11: 185–189.
- Sagi O, Rokach L. 2018. Ensemble learning: a survey. *Wiley Interdisciplinary Reviews: Data Mining and Knowledge Discovery* 8: e1249.
- Šantrůčková H, Kotas P, Bárta J, Ulrich T, Čapek P, Palmtag J, Eloy Alves RJ, Biais C, Diáková K, Gentsch N *et al.* 2018. Significance of dark CO<sub>2</sub> fixation in arctic soils. *Soil Biology and Biochemistry* 119: 11–21.
- Schmidt O, Dyckmans J, Schrader S. 2016. Photoautotrophic microorganisms as a carbon source for temperate soil invertebrates. *Biology Letters* 12: e20150646.
- Seppely CVW, Singer D, Dumack K, Fournier B, Belbahri LL, Mitchell EAD, Lara E. 2017. Distribution patterns of soil microbial eukaryotes suggests widespread algalivory by phagotrophic protists as an alternative pathway for nutrient cycling. *Soil Biology and Biochemistry* 112: 68–76.
- Shimmel SM, Darley WM. 1985. Productivity and density of soil algae in an agricultural system. *Ecology* 66: 1439–1447.
- Spohn M, Müller K, Höschen C, Mueller CW, Marhan S. 2019. Dark microbial CO<sub>2</sub> fixation in temperate forest soils increases with CO<sub>2</sub> concentration. *Global Change Biology* 26: 1926–1935.
- Wu X, Ge T, Wang W, Yuan H, Wegner C-E, Zhu Z, Whiteley AS, Wu J. 2015. Cropping systems modulate the rate and magnitude of soil microbial autotrophic CO<sub>2</sub> fixation in soil. *Frontiers in Microbiology* 6: e379.
- Wyatt KH, Turetsky MR, Rober AR, Giroldo D, Kane ES, Stevenson RJ. 2011. Contributions of algae to GPP and DOC production in an Alaskan fen: effects of historical water table manipulations on ecosystem responses to a natural flood. *Oecologia* 169: 821–832.
- Wyatt KH, Turetsky MR. 2015. Algae alleviate carbon limitation of heterotrophic bacteria in a boreal peatland. *Journal of Ecology* 103: 1165–1171.
- Xu L, Saatchi SS, Yang Y, Yu Y, White L. 2016. Performance of non-parametric algorithms for spatial mapping of tropical forest structure. *Carbon Balance and Management* 11: 14–18.
- Xu X, Thornton PE, Post WM. 2013. A global analysis of soil microbial biomass carbon, nitrogen and phosphorus in terrestrial ecosystems. *Global Ecology and Biogeography* 22: 737–749.
- Yoshitake S, Uchida M, Koizumi H, Kanda H, Nakatsubo T. 2010. Production of biological soil crusts in the early stage of primary succession on a High Arctic glacier foreland. *New Phytologist* 186: 451–460.



Yuan H, Ge T, Chen C, O'Donnell AG, Wu J. 2012. Significant role for microbial autotrophy in the sequestration of soil carbon. *Applied and Environmental Microbiology* 78: 2328–2336.

Zhang H, Zimmerman J, Nettleton D, Nordman DJ. 2020. Random forest prediction intervals. *American Statistician* 74: 392–406.

Zhao M, Heinsch FA, Nemani RR, Running SW. 2005. Improvements of the MODIS terrestrial gross and net primary production global data set. *Remote Sensing of Environment* 95: 164–176.

## Supporting Information

Additional Supporting Information may be found online in the Supporting Information section at the end of the article.

**Fig. S1** Methodological effects on soil algal abundance and net primary productivity.

**Fig. S2** Proportion of C respired during photosynthesis by soil algae.

**Fig. S3** Predictor variable reduction.

**Fig. S4** Predictive performance of different machine-learning models in predicting soil algal net primary productivity.

**Fig. S5** Workflow of Random Forest model cross-validation strategies.

**Fig. S6** Semivariograms showing the spatial autocorrelation within Random Forest model inputs variables and residuals.

**Fig. S7** Global maps of soil algal net primary productivity.

**Fig. S8** The extent of interpolation and extrapolation across all terrestrial pixels in the six best global predictive layers.

**Fig. S9** Relationships between main environmental predictors and the total density and net primary productivity of soil algae.

**Fig. S10** Random Forest model validation for predicting soil algal net primary productivity.

**Fig. S11** Random Forest out-of-bag (OOB) prediction interval.

**Fig. S12** PVS *k*-fold cross-validations.

**Fig. S13** *K*-fold model cross-validations.

**Fig. S14** Size *k*-fold CV statistics.

**Fig. S15** Low-resolution global map of annual soil algal net primary productivity.

**Fig. S16** Chlorophyll biomass of soil algae and terrestrial plants.

**Table S1** Summary of the data on soil algal abundance.

**Table S2** Summary of the data on soil algal net primary production.

**Table S3** Global covariates layers for geospatial modelling.

**Table S4** Machine learning models tested.

**Table S5** Data on plant and soil algal chlorophyll content.

Please note: Wiley Blackwell are not responsible for the content or functionality of any Supporting Information supplied by the authors. Any queries (other than missing material) should be directed to the *New Phytologist* Central Office.



## About *New Phytologist*

- *New Phytologist* is an electronic (online-only) journal owned by the New Phytologist Foundation, a **not-for-profit organization** dedicated to the promotion of plant science, facilitating projects from symposia to free access for our Tansley reviews and Tansley insights.
- Regular papers, Letters, Viewpoints, Research reviews, Rapid reports and both Modelling/Theory and Methods papers are encouraged. We are committed to rapid processing, from online submission through to publication 'as ready' via *Early View* – our average time to decision is <23 days. There are **no page or colour charges** and a PDF version will be provided for each article.
- The journal is available online at Wiley Online Library. Visit **www.newphytologist.com** to search the articles and register for table of contents email alerts.
- If you have any questions, do get in touch with Central Office (np-centraloffice@lancaster.ac.uk) or, if it is more convenient, our USA Office (np-usaoffice@lancaster.ac.uk)
- For submission instructions, subscription and all the latest information visit **www.newphytologist.com**